Eur. J. Mineral.
2010, **22**, 459–467

Qingheiite-(Fe^{2+}), $Na_2Fe^{2+}MgAl(PO_4)_3$, a new phosphate mineral from the Sebastião Cristino pegmatite, Minas Gerais, Brazil

FRÉDÉRIC HATERT[1,*], MAXIME BAIJOT[1], SIMON PHILIPPO[2] and JOHAN WOUTERS[3]

[1] Laboratoire de Minéralogie, B18, Université de Liège, 4000 Sart-Tilman, Belgium
*Corresponding author, e-mail: fhatert@ulg.ac.be
[2] Section Géologie/Minéralogie, Musée national d'histoire naturelle, Rue Münster 25, 2160 Luxembourg, Luxembourg
[3] Laboratoire de Chimie Biologique Structurale, Département de Chimie, Facultés Universitaires Notre-Dame de la Paix (FUNDP), Rue de Bruxelles 61, 5000 Namur, Belgium

Abstract: Qingheiite-(Fe^{2+}), ideally $Na_2Fe^{2+}MgAl(PO_4)_3$, is a new mineral species from the Sebastião Cristino pegmatite, Minas Gerais, Brazil. It occurs as rims around frondelite grains, included in a matrix of quartz and albite. Frondelite is locally replaced by jahnsite, cyrilovite and Fe-Mn oxides. Qingheiite-(Fe^{2+}) is transparent and exhibits a dark green colour, with a resinous lustre and with a pale to bottle green streak. It is non-fluorescent, brittle, and shows a perfect {010} cleavage. The estimated Mohs hardness is 4. The measured density is 3.6(2) g/cm^3; the calculated density is 3.54 g/cm^3. Qingheiite-(Fe^{2+}) is biaxial negative, with $\alpha = 1.692(5)$, $\beta = 1.718(3)$, and $\gamma = 1.720(5)$ (with $\lambda = 590$ nm). Pleochroism is from pale pinkish brown (*X*) to pale green (*Y*) and pale bluish grey (*Z*). The calculated $2V$ angle is 31°, and a strong dispersion r > v has been observed. The β index is parallel to the *b* crystallographic axis; α and γ lie in the (010) plane. Electron microprobe analyses gave P_2O_5 46.51, Al_2O_3 6.94, Fe_2O_3 10.58, FeO 11.46, MgO 6.32, MnO 11.23, CaO 0.24, Na_2O 6.27, K_2O 0.01, total 99.56 wt. %. The resulting empirical formula, calculated on the basis of 3 P, is $(\square_{0.65}Na_{0.35})_{\Sigma 1.00}(Na_{0.58}Mn^{2+}_{0.40}Ca_{0.02})_{\Sigma 1.00}(Fe^{2+}_{0.68}Mn^{2+}_{0.32})_{\Sigma 1.00}(Mg_{0.72}Fe^{3+}_{0.23}Fe^{2+}_{0.05})_{\Sigma 1.00}(Al_{0.62}Fe^{3+}_{0.38})_{\Sigma 1.00}[PO_4]_3$. The single-crystal unit-cell parameters are $a = 11.910(2)$, $b = 12.383(3)$, $c = 6.372(1)$ Å, $\beta = 114.43(3)°$, and $V = 855.6(3)$ Å^3, space group $P2_1/n$. The eight strongest lines in the powder X-ray diffraction pattern [*d*(in Å)(*I*)(*hkl*)] are: 3.468(35)(310), 3.047(100)(11$\overline{2}$), 2.849(80)(31$\overline{2}$), 2.810(35)(22$\overline{2}$), 2.711(40)(330), 2.688(90)(240), 2.500(40)(13$\overline{2}$; 112), 2.074(30)(31$\overline{3}$). Qingheiite-(Fe^{2+}) is the Fe^{2+} analogue of qingheiite, and belongs to the wyllieite group of minerals. The crystal structure has been refined, based on single-crystal X-ray diffraction data, to $R_1 = 2.91\%$. The mineral species and name were approved by the Commission on New Minerals, Nomenclature and Classification of the International Mineralogical Association (CNMNC-IMA) under number 2009-076.

Key-words: Qingheiite-(Fe^{2+}), new mineral, phosphate, wyllieite group, Minas Gerais, Brazil.

1. Introduction

In Brazil occurs one of the most important pegmatite provinces in the world, the Eastern Brazilian Pegmatite Province (EBPP). This province is located at the East side of the Saõ Francisco craton, mainly in the state of Minas Gerais, but it encompasses also the states of Bahia, Espírito Santo and Rio de Janeiro (Paiva, 1946; Putzer, 1976; Correia Nevez *et al*., 1986). According to Atencio (2000, 2008), 38 valid mineral species were first described in Minas Gerais, among which 15 from the Conselheiro Pena district (Galiléia, Divino das Laranjeiras, Mendes Pimentel, Linópolis).

In September 2008, M.B., F.H. and S.P. visited several pegmatites located in the Conselheiro Pena district, between Galiléia and Mendes Pimentel, in order to investigate the petrography of phosphate minerals and their relationships with associated silicates. Preliminary results obtained from this study allow to better characterize the chemistry and petrography of phosphates from the Sapucaia and Boca Rica pegmatites, and to elaborate a model explaining their genesis (Baijot *et al*., 2009).

In a sample from the Sebastião Cristino pegmatite, we observed a conspicuous petrographic feature involving two minerals: a reddish phosphate surrounded by a brownish rim. Electron-microprobe and powder X-ray diffraction analyses indicated that the core is constituted by frondelite, whereas the rim corresponds to a mineral of the wyllieite group. A single-crystal structure refinement showed that this wyllieite-type phosphate contained Mg dominant on the M(2b) site, and Fe^{2+} dominant on the M(1) site, thus corresponding to the Fe^{2+}-equivalent of qingheiite, $Na_2MnMgAl(PO_4)_3$.

Qingheiite-(Fe^{2+}), ideally $Na_2Fe^{2+}MgAl(PO_4)_3$, was accepted by the Commission on New Minerals,

0935-1221/10/0022-2030 $ 4.05
DOI: 10.1127/0935-1221/2010/0022-2030

Nomenclature and Classification of the International Mineralogical Association (CNMNC-IMA), under number IMA 2009-076. The name is in accordance with the nomenclature of the wyllieite group established by Moore & Ito (1979), and with the CNMNC-IMA guidelines which promote the use of chemical suffixes (Burke, 2008). Type specimens are stored in the collections of the Laboratory of Mineralogy, University of Liège, Belgium (n° 20381), and in the collections of the Natural History Museum, Luxembourg (n° PP022T).

2. Geological setting

The Eastern Brazilian Pegmatite Province (EBPP) is divided into several districts, among which the Conselheiro Pena district (Pedrosa-Soares *et al*., 2009) where qingheiite-(Fe^{2+}) has been found. This district mainly consists of a gneissic and migmatitic basement which is dated from Archean to Lower Proterozoic (Procrane and Piedade complex; Nalini *et al.*, 2000). The Later Proterozoic cover consists of amphibolite-facies rocks like sillimanite-staurolite-garnet-mica-bearing schists (Rio Doce Group) with intercalations of sericitic quartzites (Crenaque Group) (Nalini, 1997; Nalini *et al.*, 2000). During the Brazilian orogeny (700–450 Ma), several pre-, syn-, and post-tectonic granitoids took place in the EBPP (Bilal *et al*., 2000) originating most pegmatites (Bilal *et al*., 2000; Morteani *et al.,* 2000). Two of these intrusions occur and crosscut the cover and the basement rocks of the Conselheiro Pena district: the Galiléia and Urucum magmatic suites which belong to the G1 and G2 supersuites, respectively (Pedrosa-Soares *et al*., 2001). The Galiléia granitoid (595 Ma) is a metaluminous suite characterized by a polydiapiric batholith consisting mainly of granodiorites and tonalites with minor granites. These rocks are associated with the precollisional magmatism of the Brazilian orogeny and have calcalkaline affinities (Nalini *et al*., 2000; Pedrosa-Soares *et al*., 2001). The Urucum suite (582 Ma) is composed by four different types of rocks: a granite bearing feldspar megacrystals (Urucum facies), a medium to coarse grained granite (Palmital facies), a tourmaline-bearing granite and a pegmatitic granite (Nalini, 1997). These rocks mainly have a peraluminous composition (S-type granite) due to the syn-collisonal character of the orogeny (Nalini *et al*., 2000; Pedrosa-Soares *et al*., 2001).

Qingheiite-(Fe^{2+}) was found in the Sebastião Cristino pegmatite, located about four kilometres SE of the Córrego Frio mine, between the town of Mendes Pimentel and Linópolis (18°42'S 41°27'W) (Fig. 1). This mine is situated in the brazilianite-producing area of the EBPP. The Sebastião Cristino pegmatite is several metres wide, and strikes northeast with a gentle northwesterly dip (Cassedanne, 1983). It occurs within the garnet-, biotite-, and sillimanite-bearing schists of the São Tomé Formation (Rio Doce group, Late Proterozoic), and is probably correlated with the Galiléia granitoid (595 My) (Nalini *et al*., 2000). The mine is now abandoned but the dumps still contain quartz, graphic microcline, albite, muscovite, schorl, almandine and beryl. Phosphate minerals also occur in these dumps, particularly fluorapatite and brazilianite.

3. Physical properties

Qingheiite-(Fe^{2+}) was observed in sample SC-34, as rims (200 μm – 1 mm thickness) around grains of frondelite (up to 1 cm in diameter). These phosphates form a dendritic assemblage with albite and quartz (Fig. 2), and frondelite is locally replaced by jahnsite, cyrilovite and Fe-Mn oxides. Qingheiite-(Fe^{2+}) is transparent and exhibits a dark green colour, with a resinous lustre and with a pale to bottle green streak. It is non-fluorescent, brittle, and shows a perfect {010} cleavage. The estimated Mohs hardness is 4. The average density measured on two grains with the Berman balance is 3.6(2) g/cm^3; the calculated density is 3.54 g/cm^3. Qingheiite-(Fe^{2+}) is biaxial negative, with $\alpha = 1.692(5)$, $\beta = 1.718(3)$, and $\gamma = 1.720(5)$ (with $\lambda = 590$ nm). Pleochroism is from pale pinkish brown (*X*) to pale green (*Y*) and pale bluish grey (*Z*). The calculated 2*V* angle is 31°, and a strong dispersion r > v has been observed. The β index is parallel to the *b* crystallographic axis; α and γ lie in the (010) plane.

4. Chemical composition

Quantitative analyses were performed with a Cameca SX-50 electron microprobe (Louvain-la-Neuve, Belgium) operating in the wavelength-dispersion mode, with an accelerating voltage of 15 kV, a beam current of 20 nA, and a beam diameter of 5 μm. The following standards were used: graftonite (P, Fe, Mn), sapphire (Al), olivine (Mg), anorthite (Ca), oligoclase (Na), and orthoclase (K). H_2O and CO_2 were not determined in line with the structural analysis (see below).

As qingheiite-(Fe^{2+}) belongs to the wyllieite group, the chemical formula was calculated on the basis of 3 P (Table 1); Fe^{2+} and Fe^{3+} were subsequently calculated to achieve 24 positive charges. The presence of both Fe^{2+} and Fe^{3+} is confirmed by the dark green colour of the mineral, which is caused by charge transfers between Fe^{2+} and Fe^{3+} in the octahedral chains of the crystal structure.

The empirical formula of qingheiite-(Fe^{2+}), deduced from the electron-microprobe analyses (Table 1), corresponds to $(\square_{0.65}Na_{0.35})_{\Sigma 1.00}(Na_{0.58}Mn^{2+}_{0.40}Ca_{0.02})_{\Sigma 1.00}(Fe^{2+}_{0.68}Mn^{2+}_{0.32})_{\Sigma 1.00}(Mg_{0.72}Fe^{3+}_{0.23}Fe^{2+}_{0.05})_{\Sigma 1.00}(Al_{0.62}\ Fe^{3+}_{0.38})_{\Sigma 1.00}[PO_4]_3$. The simplified and idealised formula is $Na_2Fe^{2+}MgAl(PO_4)_3$, which requires: P_2O_5 48.61, Al_2O_3 11.64, MgO 9.20, FeO 16.40, Na_2O 14.15, total 100.00 wt.%.

5. X-ray structural investigation

The powder X-ray diffraction pattern of qingheiite-(Fe^{2+}), given in Table 2, was obtained with a PHILIPS PW-3710

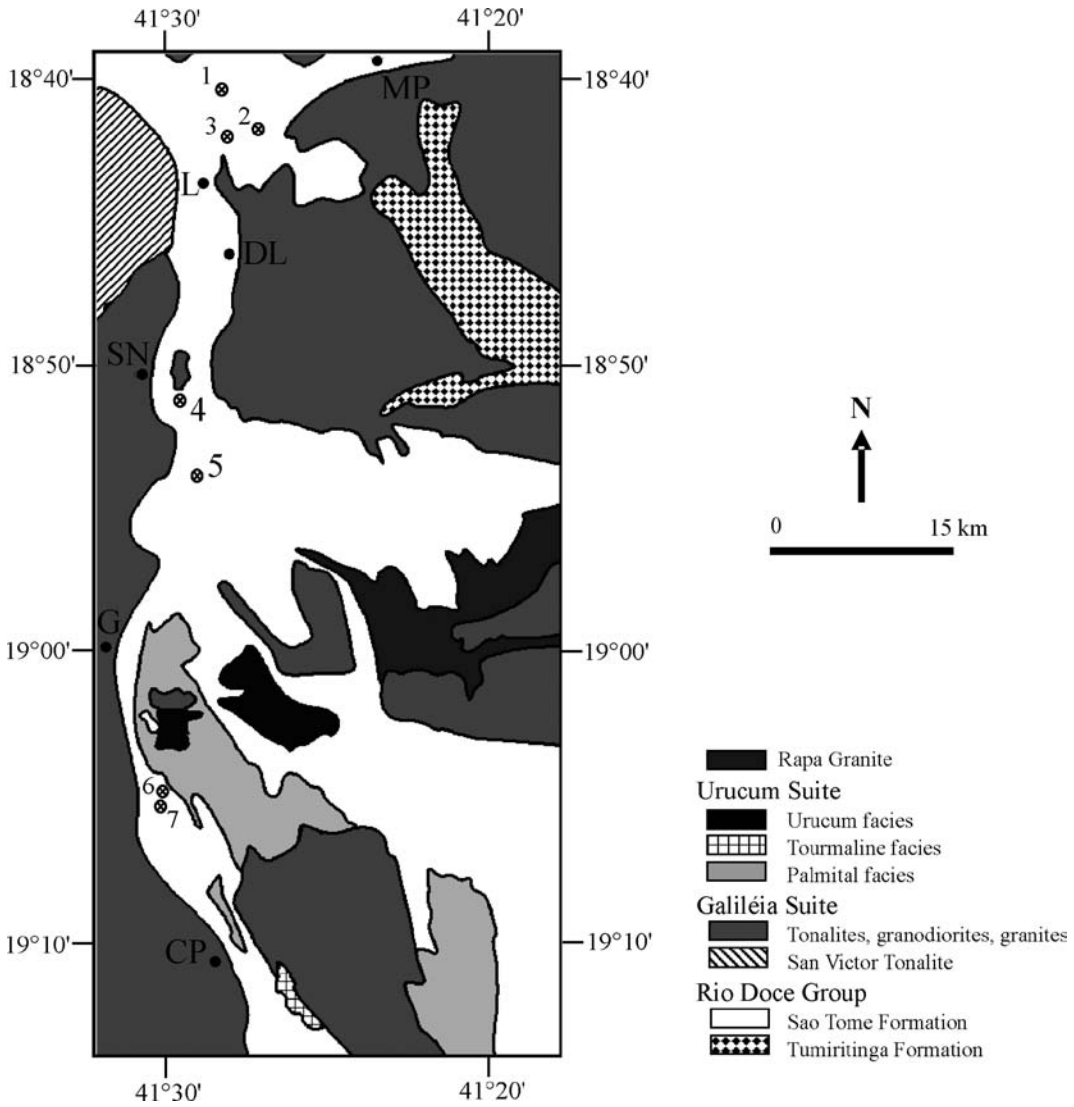

Fig. 1. Geological map of Conselheiro Pena District (modified from Nalini *et al*., 2000; Chaves *et al*., 2005; Chaves & Scholz, 2008). Localities: MP = Mendes Pimentel, L = Linópolis, DL = Divino das Larenjeiras, SN = Sapucaia do Norte, G = Galiléia, CP = Conselheiro Pena. Investigated pegmatites: 1 = Telírio, 2 = Sebastião Cristino, 3 = Jaime, 4 = Boca Rica, 5 = Sapucaia, 6 = Jocão, 7 = Noa Boa Vista.

diffractometer using Fe$K\alpha$ radiation ($\lambda = 1.9373$Å). This powder pattern is similar to those of phosphates of the wyllieite group. On the basis of the *d*-spacings shown in Table 2, which were calibrated with a $Pb(NO_3)_2$ internal standard, the least-squares refinement program LCLSQ 8.4 (Burnham, 1991) has served to calculate the unit-cell parameters $a = 11.878(3)$, $b = 12.379(4)$, $c = 6.368(2)$Å, and $\beta = 114.42(2)^\circ$.

The X-ray structural study was carried out on an Oxford Diffraction Gemini PX Ultra 4-circle diffractometer equipped with a Ruby CCD-area detector (FUNDP, Namur, Belgium), on a crystal fragment measuring $0.45 \times 0.40 \times 0.30$ mm. 217 frames with a spatial resolution of 1° were collected by the ϕ/ω scan technique, with a counting time of 1.5 s per frame, in the range $7.00^\circ < 2\theta < 61.18^\circ$. A total of 4983 reflections were extracted from these frames, corresponding to 2377 unique reflections. The unit-cell parameters refined from these reflections, $a = 11.910(2)$, $b = 12.383(3)$, $c = 6.372(1)$Å, and $\beta = 114.43(3)^\circ$, are in good agreement with those refined from the X-ray powder data (see above). Data were corrected for Lorenz, polarisation and absorption effects, the latter with an empirical method using the SCALE3 ABSPACK scaling algorithm included in the CrysAlisRED package (Oxford Diffraction, 2007).

The structure of qingheiite-(Fe^{2+}) (Fig. 3) was refined in space group $P2_1/n$. The starting atomic coordinates were those of rosemaryite from the Buranga pegmatite, Rwanda (Hatert *et al*., 2006), and scattering curves for neutral atoms, together with anomalous dispersion corrections, were taken from the *International Tables for X-ray Crystallography, Vol. C* (Wilson, 1992). For the sake of simplicity, Ca and K, which occur in low to trace amounts, were not taken into account in the crystal-structure refinement. Finally, the relative occupancies of Na and vacancies on X(2) and X(1b), of Fe and Na on M(1), of Al and Fe on M(2a), and of Fe and Mg on M(2b), were

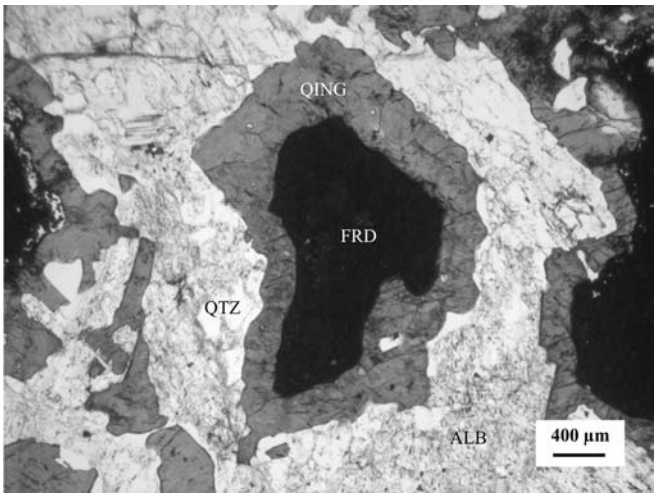

Fig. 2. Rim of qingheiite-(Fe^{2+}) (QING) surrounding frondelite (FRD) in a quartz (QTZ)-albite (ALB) matrix. Plane polarized light, sample SC-34.

refined. As the refined scattering of the X(1a) site was close to 25 electrons, the X(1a) occupancy was constrained to 1.0 Mn. The refinement was completed using anisotropic displacement parameters for all atoms. The final conventional R_1 factor ($F_0 > 2\sigma$ (F_0)) is 0.0239. Further details of the intensity data collection and refinement are given in Table 3.

6. Discussion

6.1. Compatibility index

The compatibility index of qingheiite-(Fe^{2+}), 1-(K_P/K_C), calculated with the measured density, is 0.021 and falls in the category ''excellent''. The compatibility obtained from the calculated density is 0.005, in the ''superior'' category according to Mandarino (1981).

Table 1. Electron-microprobe analysis of qingheiite-(Fe^{2+}).

Constituent	wt%	Range	Standard deviation	Number of cations
P_2O_5	46.51	46.07–47.20	0.45	3.000
Al_2O_3	6.94	6.58–7.10	0.19	0.623
Fe_2O_3[a]	10.58	9.14–14.89	2.16	0.607
FeO[a]	11.46	7.93–12.51	1.72	0.730
MgO	6.32	6.24–6.39	0.06	0.718
MnO	11.23	10.98–11.40	0.16	0.725
CaO	0.24	0.14–0.33	0.06	0.020
Na_2O	6.27	5.92–6.43	0.19	0.927
K_2O	0.01	0.00–0.04	0.02	0.001
Total	99.56			

Note: Analyst J. Wautier; average of 6 point analyses. Numbers of cations were calculated on the basis of 3 P per formula unit.
[a]Fe_2O_3 and FeO contents were calculated to achieve 24 charges per 3 P formula unit.

Table 2. Indexed X-ray powder-diffraction pattern of qingheiite-(Fe^{2+}).

$I_{obs.}$	$d_{obs.}$(Å)	$d_{calc.}$(Å)	$h\,k\,l$
15	8.19	8.145	1 1 0
20	6.19	6.190	0 2 0
15	5.43	5.408	2 0 0
35	3.468	3.461	3 1 $\bar{0}$
100	3.047	3.048	1 1 $\bar{2}$
10	3.013	3.012	1 3 1
15	2.897	2.899	0 0 $\bar{2}$
80	2.849	2.848	3 1 $\bar{2}$
35	2.810	2.811	2 2 $\bar{2}$
15	2.729	2.730	0 4 1
40	2.711	2.715	3 3 0
90	2.688	2.686	2 4 0
15	2.626	2.626	0 2 2
10	2.589	2.590	2 3 1
40	2.500	2.499	1 3 $\bar{2}$; 1 1 2
10	2.384	2.384	3 3 $\bar{2}$; 4 2 $\bar{2}$
5	2.305	2.305	1 5 $\bar{1}$
5	2.210	2.209	2 4 $\bar{2}$; 3 3 1
15	2.169	2.169	2 1 2; 1 3 2
15	2.127	2.126	3 4 $\bar{2}$
30	2.074	2.074	3 1 $\bar{3}$
20	2.041	2.041	3 5 0
10	1.966	1.968	1 4 2
10	1.916	1.916	4 2 $\bar{3}$; 5 3 0
10	1.845	1.845	0 2 3
5	1.801	1.803	6 0 0
5	1.748	1.748	2 4 $\bar{3}$; 6 3 $\bar{2}$
5	1.732	1.731	3 3 2
5	1.651	1.652	6 3 0
5	1.638	1.638	6 4 $\bar{2}$

6.2. Structural features

Final positional parameters for qingheiite-(Fe^{2+}) are given in Table 4, whereas selected bond distances are reported in Table 5. Anisotropic displacement parameters

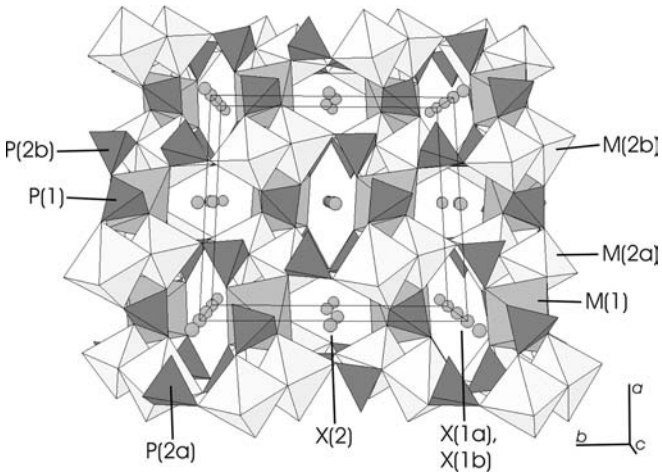

Fig. 3. Projection of the crystal structure of qingheiite-(Fe^{2+}). The PO_4 tetrahedra are dark grey, the M(1) octahedra are light grey, and the M(2a) and M(2b) octahedra are white. The circles indicate Na and Mn on the X(1a), X(1b), and X(2) crystallographic sites.

Table 3. Experimental details for the single-crystal X-ray diffraction study of qingheiite-(Fe^{2+}).

Dimensions of the crystal (mm)	ca. 0.45 × 0.40 × 0.30
a (Å)	11.910(2)
b (Å)	12.383(3)
c (Å)	6.372(1)
β (°)	114.43(3)°
Vol. (Å^3)	855.6(3)
Space group	$P2_1/n$
Z	4
Diffractometer	Oxford Diffraction Gemini PX Ultra with Ruby CCD-area detector
Operating conditions	50 kV, 40 mA
Radiation	Mo$K\alpha$ ($\lambda = 0.71073$ Å)
Scan mode	ϕ/ω scan
$2\theta_{min.}$, $2\theta_{max}$	7.00°, 61.18°
Range of indices	$-6 \leq h \leq 9$, $-16 \leq k \leq 15$, $-10 \leq l \leq 15$
Measured intensities	4983
Unique reflections	2377
Observed [$I > 2\sigma(I)$] reflections	2113
Absorption correction	Empirical (SCALE3 ABSPACK scaling algorithm)
μ (mm^{-1})	4.093
l.s. refinement program	SHELXL-97 (Sheldrick, 2008)
Refined parameters	192
R_1 ($F_o > 2\sigma(F_o)$)	0.0239
R_1 (all)	0.0291
wR_2 (all)	0.0603
S (goodness of fit)	1.142
Max Δ/σ in the last l.s. cycle	0.000
Max peak and hole in the final ΔF map (e/Å^3)	+0.40 and –0.58

are compiled in Table S1, freely available online as Supplementary material on the GSW website of the journal (http:///eurjmin.geoscienceworld.org/), and the Fo − Fc table is available from the first author. The basic features of the crystal structure of qingheiite-(Fe^{2+}) (Fig. 3) are identical to those of the other members of the wyllieite group. They consist of kinked chains of edge-sharing octahedra stacked parallel to {101}. These chains are formed by a succession of M(2a)-M(2b) octahedral pairs, linked by highly distorted M(1) octahedra. Equivalent chains are connected in the b direction by the P(1), P(2a) and P(2b) phosphate tetrahedra to form sheets oriented perpendicular to [010]. These interconnected sheets produce channels parallel to c, channels that contain the large X sites.

The X(1a) site of qingheiite-(Fe^{2+}) is a distorted octahedron, whereas the X(1b) site can be described as a very distorted cube. The morphology of the X(2) site corresponds to very distorted gable disphenoid with a [7 + 1] coordination, similar to the X(2) site of rosemaryite (Hatert *et al*., 2006) and to the A(2)' site of the alluaudite structure (Hatert *et al*., 2000).

A detailed cationic distribution was established, in order to obtain a better agreement with the chemical composition of qingheiite-(Fe^{2+}) (Table 1). The results given in Table 6 indicate that the refined site populations (RSP), obtained from the single-crystal structure refinement, are in good agreement with the assigned site populations (ASP) deduced from the chemical data. Moreover, the refined site-scattering values (RSS) and the mean bond lengths (MBL), obtained from the structure refinement, are very close to the calculated site scattering values (CSS) and the calculated bond lengths (CBL), respectively (Table 6). This agreement confirms the reliability of the assigned site populations.

Finally, the bond valence table for qingheiite-(Fe^{2+}) is presented in Table 7, where the bond valence sums were calculated according to values of Brown & Altermatt (1985). The bond valences for O and P atoms are very close to the theoretical values of 2.00 and 5.00, respectively (Table 7). Concerning the cationic sites, a good correspondence between the theoretical and the calculated values is generally observed.

6.3. Nomenclature remarks

Qingheiite-(Fe^{2+}) belongs to the wyllieite group of minerals, group 8.AC.15 according to Nickel & Strunz (2001). In this group, when M(1) is occupied by Mn, the mineral name depends on the cation that occupies the M(2b) site (M(2a) in ferrowyllieite) (Moore & Ito, 1979; Hatert *et al*., 2005 2006): wyllieite (Fe^{2+}), rosemaryite (Fe^{3+}), or qingheiite (Mg). The prefix ''ferro-'' is then added if the M(1) site is occupied by Fe^{2+}, as in ferrowyllieite or in ferrorosemaryite. The mineral investigated herein contains Mg as the dominant cation on the M(2b) site, and Fe^{2+} as the dominant cation on the M(1) site (Table 6). It should consequently be named ''ferroqingheiite'', but the name qingheiite-(Fe^{2+}) was chosen according to the current CNMNC suffix-type nomenclature (Burke, 2008). Qingheiite-(Fe^{2+}) corresponds to a qingheiite with the M(1) site predominantly occupied by Fe^{2+}. A comparison between the properties of the different species included in the wyllieite group of minerals is given in Table 8.

The structural formula of qingheiite-(Fe^{2+}), calculated from the assigned site populations (Table 6), corresponds to $(Na_{0.18}Mn_{0.15}Ca_{0.02}\square_{0.65})(Na_{0.50}Mn_{0.50})(Fe^{2+}_{0.52}Na_{0.25}Fe^{3+}_{0.16}Mn_{0.07})(Al_{0.62}Mg_{0.28}Fe^{3+}_{0.10})(Mg_{0.44}Fe^{3+}_{0.35}Fe^{2+}_{0.21})(PO_4)_3$. This formula is comparable to the empirical formula obtained from the electron-microprobe analyses, $(\square_{0.65}Na_{0.35})(Na_{0.58}Mn_{0.40}Ca_{0.02})(Fe^{2+}_{0.68}Mn_{0.32})(Mg_{0.72}Fe^{3+}_{0.23}Fe^{2+}_{0.05})(Al_{0.62}Fe^{3+}_{0.38})(PO_4)_3$ (Table 1). As can be seen from these two formulae, significant vacancy occurs on the X(2) site. These vacancies are introduced in the crystal structure of qingheiite-(Fe^{2+}) *via* the two substitution mechanisms $^{X2}Na^+ + {}^{M2b}Fe^{2+} = {}^{X2}\square + {}^{M2b}Fe^{3+}$ and $^{X2}Na^+ + {}^{X1a,X1b}Na^+ = {}^{X2}\square + {}^{X1a,X1b}(Mn^{2+}, Ca)$. Even if each of these independent substitution mechanisms does not extend beyond the 50% boundary, the total vacancy on X(2) is very large. The first substitution mechanism extends up to about 23% (0.23 Fe^{3+} on M(2b)), and the second substitution mechanism to about 42% (0.42 Mn + Ca on X(1a) + X(1b)). The total contribution of both mechanisms should

Table 4. Final fractional coordinates and equivalent displacement parameters (Å^2) for qingheiite-(Fe^{2+}).

Site	Atom	*x*	*y*	*z*	U_{eq}
X(2)	Na[a]	0.0005(2)	−0.0172(2)	0.2483(3)	0.0317(8)
X(1a)	Mn[b]	0.5	0	0	0.0110(1)
X(1b)	Na[c]	0.5	0	0.5	0.0206(5)
M(1)	Fe[d]	0.00083(3)	0.26084(3)	0.26527(5)	0.0099(1)
M(2a)	Al[e]	0.28215(5)	−0.33551(5)	0.36006(9)	0.0075(2)
M(2b)	Fe[f]	0.22407(4)	−0.14767(3)	0.62912(7)	0.0077(1)
P(1)	P	0.00633(5)	−0.28560(4)	0.23900(8)	0.0071(1)
P(2a)	P	0.23910(5)	−0.09798(4)	0.11758(9)	0.0080(1)
P(2b)	P	0.24058(5)	0.11455(4)	0.64754(9)	0.0077(1)
O(1a)	O	0.4494(1)	−0.2828(1)	0.5156(2)	0.0109(3)
O(1b)	O	0.4550(1)	−0.7109(1)	0.0508(2)	0.0100(3)
O(2a)	O	0.1107(1)	−0.3511(1)	0.2200(3)	0.0136(3)
O(2b)	O	0.0828(1)	−0.6277(1)	0.7435(2)	0.0121(3)
O(3a)	O	0.3189(1)	−0.3264(1)	0.0873(2)	0.0117(3)
O(3b)	O	0.3395(1)	−0.6548(1)	0.6130(2)	0.0118(3)
O(4a)	O	0.1257(1)	0.4118(1)	0.3513(2)	0.0116(3)
O(4b)	O	0.1189(1)	−0.3998(1)	0.7763(2)	0.0111(3)
O(5a)	O	0.2368(1)	−0.1676(1)	0.3166(2)	0.0134(3)
O(5b)	O	0.2226(1)	−0.8148(1)	0.8312(2)	0.0111(3)
O(6a)	O	0.3169(2)	−0.4865(1)	0.3811(3)	0.0159(3)
O(6b)	O	0.3224(2)	−0.4938(1)	0.8776(3)	0.0151(3)

Note: Refined sites occupancies:
[a]0.573(6) Na + 0.427(6)□.
[b]0.500 Mn.
[c]0.476(6) Na + 0.024(6)□.
[d]0.868(3) Fe + 0.132(3) Na.
[e]0.925(3) Al + 0.075(3) Fe.
[f]0.536(3) Fe + 0.464(3) Mg.

theoretically produce 0.65 vacancies *pfu*, in perfect agreement with the 0.65 vacancies observed on X(2).

Even if vacancies are dominant on X(2) due to the intervention of these substitution mechanisms, the ideal formula of qingheiite-(Fe^{2+}) is $Na_2Fe^{2+}MgAl(PO_4)_3$, in which Na is dominant on X(2). This Na-dominancy is necessary to maintain charge balance, and can be justified since none of the involved substitution mechanisms extends beyond the 50% boundary (Hatert & Burke, 2008). It is noteworthy that in the wyllieite group, the X(1a) and X(1b) sites are grouped together for nomenclature purposes, according to the CNMNC guidelines of Hatert & Burke (2008). This grouping is necessary since these two sites show similar crystal-chemical behaviour.

In the literature, five crystal-structure refinements on wyllieite-type compounds are available: ferrowyllieite (Moore & Molin-Case, 1974), qingheiite (Zhesheng *et al*., 1983), ferrorosemaryite (Hatert *et al*., 2005), rosemaryite (Hatert *et al*., 2006), and synthetic $Na_{1.265}Mn^{2+}_{2.690}Mn^{3+}_{0.785}(PO_4)_3$ (Yakubovich *et al*., 2005). The distribution of Mg and Al between the M(2a) and M(2b) crystallographic sites of qingheiite-(Fe^{2+}) is similar to that observed in qingheiite (Zhesheng *et al*., 1983), with Al dominant on M(2a) and Mg dominant on M(2b) (Table 6). Al is also dominant on the M(2a) site of ferrorosemaryite (Hatert *et al*., 2005) and of rosemaryite (Hatert *et al*., 2006), whereas this site is predominantly occupied by Fe^{2+} in ferrowyllieite (Moore & Molin-Case, 1974). This different distribution is certainly

Table 5. Selected bond distances (Å) and angles (°) for qingheiite-(Fe^{2+}).

P(1)-O(2a)	1.530(2)	X(2)-O(6b)'	2.461(3)
P(1)-O(1b)	1.533(2)	X(2)-O(6a)	2.462(3)
P(1)-O(2b)	1.546(2)	X(2)-O(6b)	2.552(3)
P(1)-O(1a)	1.551(2)	X(2)-O(1b)	2.658(3)
Mean	1.540	X(2)-O(6a)'	2.677(3)
		X(2)-O(3b)	2.749(2)
O(2a)-P(1)-O(1b)	115.35(9)	X(2)-O(1a)	2.831(3)
O(2a)-P(1)-O(2b)	104.00(9)	X(2)-O(3a)	3.072(2)
O(2a)-P(1)-O(1a)	106.10(9)	Mean	2.683
O(1b)-P(1)-O(2b)	108.87(8)		
O(1b)-P(1)-O(1a)	109.41(9)	X(1a)-O(4b) × 2	2.141(2)
O(2b)-P(1)-O(1a)	113.14(9)	X(1a)-O(2b) × 2	2.148(2)
Mean	109.48	X(1a)-O(4a) × 2	2.347(2)
		Mean	2.212
P(2a)-O(6a)	1.535(2)		
P(2a)-O(4a)	1.543(2)	X(1b)-O(2a) × 2	2.361(2)
P(2a)-O(5a)	1.543(2)	X(1b)-O(4a) × 2	2.382(2)
P(2a)-O(3b)	1.547(2)	X(1b)-O(4b) × 2	2.692(2)
Mean	1.542	X(1b)-O(2b) × 2	2.734(2)
		Mean	2.542
O(4a)-P(2a)-O(6a)	111.20(9)		
O(4a)-P(2a)-O(5a)	108.10(9)	M(1)-O(1a)	2.173(2)
O(4a)-P(2a)-O(3b)	110.33(9)	M(1)-O(4b)	2.180(2)
O(6a)-P(2a)-O(5a)	110.00(9)	M(1)-O(1b)	2.194(2)
O(6a)-P(2a)-O(3b)	108.70(9)	M(1)-O(3b)	2.194(2)
O(5a)-P(2a)-O(3b)	108.47(9)	M(1)-O(3a)	2.235(2)
Mean	109.47	M(1)-O(4a)	2.310(2)
		Mean	2.214

Table 5. Continued.

P(2b)-O(6b)	1.513(2)		
P(2b)-O(5b)	1.545(2)	M(2a)-O(2a)	1.870(2)
P(2b)-O(4b)	1.548(2)	M(2a)-O(6a)	1.908(2)
P(2b)-O(3a)	1.549(2)	M(2a)-O(1a)	1.935(2)
Mean	1.539	M(2a)-O(3a)	1.963(2)
		M(2a)-O(5b)	2.008(2)
O(6b)-P(2b)-O(4b)	110.85(9)	M(2a)-O(5a)	2.137(2)
O(6b)-P(2b)-O(3a)	107.93(9)	Mean	1.970
O(6b)-P(2b)-O(5b)	111.35(9)		
O(4b)-P(2b)-O(3a)	111.10(9)	M(2b)-O(6b)	1.980(2)
O(4b)-P(2b)-O(5b)	107.34(9)	M(2b)-O(5a)	2.073(2)
O(3a)-P(2b)-O(5b)	108.27(8)	M(2b)-O(3b)	2.076(2)
Mean	109.47	M(2b)-O(1b)	2.111(2)
		M(2b)-O(2b)	2.114(2)
		M(2b)-O(5b)	2.149(2)
		Mean	2.084

due to the effective ionic radius of Fe^{2+} (0.780Å; Shannon, 1976), significantly larger than those of Fe^{3+} (0.645Å) and Mg (0.720Å) (Hatert *et al.*, 2006).

6.4. Genetic considerations

In the Sebastião Cristino pegmatite, qingheiite-(Fe^{2+}) appears as rims around frondelite grains included in an albite-quartz matrix (Fig. 2). Since minerals of the rockbridgeite–frondelite series generally crystallize under oxidizing conditions during the hydration stage of the phosphate minerals alteration sequence (Fransolet, 1976; Keller & Von Knorring, 1989; Roda *et al.*, 1998), it is likely that frondelite from Sebastião Cristino is an oxidation product of primary triphylite. Rims of qingheiite-(Fe^{2+}) consequently result from a reaction between this primary, and

Table 6. Refined site populations (RSP, *apfu*), refined site-scattering values (RSS, *epfu*), mean bond-lengths (MBL, Å), assigned site populations (ASP, *apfu*), calculated site-scattering values (CSS, *epfu*), and calculated bond lengths (CBL, Å) for qingheiite-(Fe^{2+}).

	Results of the structure determination			Results of the chemical analysis		
Site	RSP	RSS	MBL	ASP	CSS	CBL[a]
X(2)	0.573 Na	6.4	2.683	0.177 Na^{+} + 0.153 Mn^{2+} + 0.020 Ca^{2+}	6.2	2.500
X(1a)	1.000 Mn	25.4	2.212	1.000 Mn^{2+}	25.0	2.230
X(1b)	0.952 Na	10.7	2.542	1.000 Na^{+}	11.0	2.600
M(1)	0.868 Fe + 0.132 Na	24.2	2.214	0.521 Fe^{2+} + 0.250 Na^{+} + 0.157 Fe^{3+} + 0.072 Mn^{2+}	22.2	2.222
M(2a)	0.925 Al + 0.075 Fe	14.1	1.970	0.623 Al^{3+} + 0.277 Mg^{2+} + 0.100 Fe^{3+}	14.0	1.997
M(2b)	0.536 Fe + 0.464 Mg	19.7	2.084	0.441 Mg^{2+} + 0.350 Fe^{3+} + 0.209 Fe^{2+}	19.8	2.106

Note: [a]The CBL values have been calculated from the ASP, assuming a full occupancy of the crystallographic sites.

Table 7. Bond-valence table (*vu*) for qingheiite-(Fe^{2+}).

	X(2)	X(1a)	X(1b)	M(1)	M(2a)	M(2b)	P(1)	P(2a)	P(2b)	$\sum$
O(1a)	0.063			0.327	0.493		1.195			2.08
O(1b)	0.100			0.308		0.353	1.255			2.02
O(2a)			0.221 [a]		0.588		1.265			2.07
O(2b)		0.381 [a]	0.081 [a]			0.348	1.215			2.02
O(3a)	0.171			0.276	0.456				1.205	2.11
O(3b)	0.079			0.309		0.386		1.208		1.98
O(4a)		0.222 [a]	0.209 [a]	0.226				1.225		1.88
O(4b)		0.388 [a]	0.090 [a]	0.322					1.205	2.00
O(5a)					0.285	0.390		1.221		1.90
O(5b)					0.406	0.317			1.212	1.93
O(6a)	0.170				0.530			1.248		2.05
O(6a)'	0.095									
O(6b)	0.133					0.502			1.325	1.99
O(6b)'	0.033									
$S_{calc.}$	0.84	1.98	1.20	1.77	2.76	2.30	4.93	4.90	4.95	
$S_{theor.}$	0.52	2.00	1.00	1.91	2.72	2.35	5.00	5.00	5.00	

Note: The bond valences were calculated from the bond lengths given in Table 5, and from the assigned site populations of Table 6, with the parameters of Brown & Altermatt (1985).
[a]Bond valences were multiplied by two, for the calculation of the valence on the X(1a) and X(1b) crystallographic sites. A full occupancy has been assumed for the X(2) site.

Table 8. Comparison of the physical properties of qingheiite-(Fe^{2+}) with those of other minerals of the wyllieite group.

	Wyllieite	Ferrowyllieite	Rosemaryite	Ferrorosemaryite	Qingheiite	Qingheiite-(Fe^{2+})
References	[a]	[b, c]	[a]	[d]	[e]	[f]
Space Group	$P2_1/n$	$P2_1/n$	$P2_1/n$	$P2_1/n$	$P2_1/n$	$P2_1/n$
a (Å)	11.967(2)	11.868(15)	11.977(2)	11.824(2)	11.856(3)	11.910(2)
b (Å)	12.462(3)	12.382(12)	12.388(2)	12.346(3)	12.411(3)	12.383(3)
c (Å)	6.409(1)	6.354(9)	6.320(1)	6.293(1)	6.421(1)	6.372(1)
β (°)	114.63(2)	114.52(8)	114.45(2)	114.32(1)	114.45(2)	114.43(3)
X	Colourless	Smoky bluish-grey	Brownish yellow	Dark green	Dark bluish green	Pale pinkish brown
Y	Greenish blue	Smoky bluish-green	Brownish yellow	Dark green to brownish	Jade green	Pale green
Z	Greenish blue	Green	Greenish yellow	Dark brown	Light yellowish green	Pale bluish grey
α	1.685(2)	1.688(2)	1.723(2)	1.730(5)	1.678	1.692(5)
β	1.688(2)	1.691(2)	1.742(2)	1.758(7)	1.684	1.718(3)
γ	1.692(2)	1.696(2)	1.758(2)	1.775(5)	1.691	1.720(5)
Optical sign	+	+	–	–	+	–
2V (°)	90	50	80	82(1)	79.6	31
Dispersion	n.g.	r < v strong	n.g.	r < v strong	r > v strong	r > v strong
D_{meas} (g/cm^3)	n.g.	3.601(3)	n.g.	n.g.	3.718	3.6(2)
D_{calc} (g/cm^3)	n.g.	3.60	n.g.	3.62	3.61	3.54

[a]Fransolet (1995).
[b]Moore & Ito (1973).
[c]Moore & Molin-Case (1974).
[d]Hatert *et al*. (2005).
[e]Zhesheng *et al*. (1983).
[f]This work; n.g.: not given.

probably Mg-bearing, triphylite (source of Fe, Mn, Mg, P) and albite from the matrix (source of Na, Al). This reaction certainly took place during the albitization stage, during which high amounts of Na are available. The oxidation processes affecting the pegmatite subsequently oxidized triphylite in ferrisicklerite and then in frondelite, and provoked an oxidation of qingheiite-(Fe^{2+}) following the substitution mechanism $Na^{+}+Fe^{2+}= \square+Fe^{3+}$. This oxidation is responsible for the presence of vacancies and Fe^{3+} in qingheiite-(Fe^{2+}) (see empirical formula). Cyrilovite and Fe-Mn-oxides crystallized later under meteoric conditions.

Acknowledgements: Many thanks are due L. Bindi, A.-M. Fransolet, M. Mellini, and P. Zanazzi for their constructive comments on the manuscript, as well as to J. Cassedanne for his help during the fieldtrip in Brazil. F.H. thanks the FRS-F.N.R.S. (Belgium) for a position of ''Chercheur qualifié'', and M.B. thanks the FNR (Luxembourg) for PhD grant TR-PHD-BFR07-137.

References

Atencio, D. (2000): Type Mineralogy of Brazil. Universidade de São Paulo, Brazil, 114 p.

— (2008): 21st-Century Brazilian Minerals. Mineralogy and Museums 6th international conference, Abstract book, 12.

Baijot, M., Hatert, F., Philippo, S., Cassedanne, J.P., Fransolet, A.-M. (2009): Mineralogy and petrography of phosphate minerals from Sapucaia and Boca Rica pegmatites, Minas Gerais, Brazil. *Estudos Geológicos*, **19**, **2**, 47–51.

Bilal, E., Horn, A.H., Nalini, H.A., Jr., Mello, F.M., Correia-Neves, J.M., Giret, A.R., Moutte, J., Fuzikawa, K., Fernandes, M.L.S. (2000): Neoproterozoic granitoid suites in southeastern Brazil. *Revista Brasileira de Geociências*, **30**, 51–54.

Brown, I.D., Altermatt, D. (1985): Bond-valence parameters obtained from a systematic analysis of the inorganic crystal structure database. *Acta Cryst*., **B41**, 244–247.

Burke, E.A.J. (2008): Tidying-up mineral names: an IMA-CNMNC scheme for suffixes, hyphens and diacritical marks. *Mineral. Rec*., **39**, 131–135.

Burnham, C.W. (1991): LCLSQ version 8.4, least-squares refinement of crystallographic lattice parameters. Department of Earth and Planetary Sciences, Harvard University, Cambridge, Massachusetts, 24 p.

Cassedanne, J.P. (1983): The Córrego Frio mine and vicinity, Minas Gerais, Brazil. *Mineral. Rec*., **14**, 227–237.

Chaves, M.L., Scholz, R. (2008): Pegmatito Gentil (Mendes Pimentel, MG) e suas paragêneses mineralógicas de fosfatos raros. . *R. Esc, Minas, Ouro Preto, Geociências*, **61**, **2**, 141–149.

Chaves, M.L., Scholz, R., Atencio, D., Karfunkel, J. (2005): Assembléias e paragêneses minerais singulares nos pegmatitos de região de Galiléia (Minas Gerais). *Geociências*, **24**, **2**, 143–161.

Correia Nevez, J.M., Pedrosa Soares, A.C., Marciano, V.R.P., da, R.O. (1986): A provincial pegmatítica oriental do Brazil à luz

dos conhecimentos atuais. *Revista Brasileira de Geociências*, **16**, 106–118.

Fransolet, A.-M. (1976): L'huréaulite: ses propriétés minéralogiques et son rôle dans l'évolution génétique des phases $Li(Fe,Mn)PO_4$. *Bull. Soc. Fr. Minéral. Cristallogr.*, **99**, 261–273.

— (1995): Wyllieite et rosemaryite dans la pegmatite de Buranga, Rwanda. *Eur. J. Mineral.*, **7**, 567–575.

Hatert, F., Burke, E.A.J. (2008): The IMA-CNMNC dominant-constituent rule revisited and extended. *Can. Mineral.*, **46**, 717–728.

Hatert, F., Keller, P., Lissner, F., Antenucci, D., Fransolet, A.-M. (2000): First experimental evidence of alluaudite-like phosphates with high Li-content: the $(Na_{1-x}Li_x)MnFe_2(PO_4)_3$ series ($x = 0$ to 1). *Eur. J. Mineral.*, **12**, 847–857.

Hatert, F., Lefèvre, P., Fransolet, A.-M., Spirlet, M.-R., Rebbouh, L., Fontan, F., Keller, P. (2005): Ferrorosemaryite, $NaFe^{2+}Fe^{3+}Al(PO_4)_3$, a new phosphate mineral from the Rubindi pegmatite, Rwanda. *Eur. J. Mineral.*, **17**, 749–759.

Hatert, F., Hermann, R.P., Fransolet, A.-M., Long, G.J., Grandjean, F. (2006): A structural, infrared, and Mössbauer spectral study of rosemaryite, $NaMnFe^{3+}Al(PO_4)_3$. *Eur. J. Mineral.*, **18**, 775–785.

Keller, P., Von Knorring, O. (1989): Pegmatites at the Okatjimukuju farm, Karibib, Namibia. Part I. Phosphate mineral associations of the Clementine II pegmatite. *Eur. J. Mineral.*, **1**, 567–593.

Mandarino, J.A. (1981): The Gladstone-Dale relationship: Part IV. The compatibility concept and its application. *Can. Mineral.*, **19**, 441–450.

Moore, P.B., Ito, J. (1973): Wyllieite, $Na_2Fe^{2+}{}_2Al(PO_4)_3$, a new species. *Mineral. Rec.*, **4**, 131–136.

Moore, P.B., Ito, J. (1979): Alluaudites, wyllieites, arrojadites: crystal chemistry and nomenclature. *Mineral. Mag.*, **43**, 227–235.

Moore, P.B., Molin-Case, J. (1974): Contribution to pegmatite phosphate giant crystal paragenesis: II. The crystal chemistry of wyllieite, $Na_2Fe^{2+}{}_2Al(PO_4)_3$, a primary phase. *Am. Mineral.*, **59**, 280–290.

Morteani, G., Preinfalk, C., Horn, A.H. (2000): Classification and mineralization potential of the pegmatites of the Eastern Brazilian Pegmatite Province. *Mineral. Deposita*, **35**, 638–655.

Nalini, H.A. (1997): Caractérisation des suites magmatiques néoprotérozoïques de la région de Conselheiro Pena et Galiléia (Minas Gerais, Brésil): étude géochimique et structurale des suites de Galiléia et Urucum et leur relation avec les pegmatites à éléments rares associées. *Unpublished PhD thesis, Ecole des mines de Saint Etienne et Ecole des mines de Paris*, 237 p.

Nalini, H.A., Bilal, E., Paquette, J.-L., Pin, C., Rômulo, M. (2000): Géochronologie U-Pb et géochimie isotopique Sr-Nd des granitoïdes néoprotérozoïques des suites Galiléia et Urucum, vallée du Rio Doce, Sud-Est du Brésil. *Comptes Rendus Acad. Sc., Sc. de la Terre et des Planètes*, **331**, 459–466.

Nickel, E.H., Strunz, H. (2001): Strunz Mineralogical Tables, 9th Edition. E. Schweizerbart'sche Verlagsbuchhandlung, Stuttgart, Germany, 870 p.

Oxford Diffraction (2007): CrysAlis CCD and CrysAlis RED, version 1.71. Oxford Diffraction, Oxford, England.

Paiva, G. de (1946): Província pegmatíticas do Brazil. *Boletim DNPM-DFMP*, **78**, 13–21.

Pedrosa-Soares, A.C., Noce, C.M., Wiedemann, C.M., Pinto, C.P. (2001): The Araçuaí-West-Congo Orogen in Brazil: an overview of confined orogen formed during Gondwanaland assembly. *Precambr. Res.*, **110**, 307–323.

Pedrosa-Soares, A.C., Chaves, M., Scholz, R. (2009): Eastern Brazilian pegmatite province. *4th International Symposium on Granitic Pegmaites, Field trip guide*, 1–28.

Putzer, H. (1976): Metallogenetische Provinzen in Südamerika. schweizerbart'sche Verlagsbuchhandlung, Stuttgart, Germany, 316 p.

Roda, E., Fontan, F., Pesquera, A., Keller, P. (1998): The Fe-Mn phosphate associations from the Pinilla de Fermoselle pegmatite, Zamora, Spain: occurrence of kryzhanovskite and natrodufrénite. *Eur. J. Mineral.*, **10**, 110–125.

Shannon, R.D. (1976): Revised effective ionic radii and systematic studies of interatomic distances in halides and chalcogenides. *Acta Cryst. A*, **32**, 751–767.

Sheldrick, G.M. (2008): A short history of *SHELX*. *Acta Cryst. A*, **64**, 112–122.

Wilson, A.J.C. (1992): International Tables for X-ray Crystallography. Vol. C, Kluwer Academic Press, London, 883 p.

Yakubovich, O.V., Massa, W., Gavrilenko, P.G., Dimitrova, O.V. (2005): The crystal structure of a new synthetic member in the wyllieite group: $Na_{1.265}Mn^{2+}{}_{2.690}Mn^{3+}{}_{0.785}(PO_4)_3$. *Eur. J. Mineral.*, **17**, 741–747.

Zhesheng, M., Nicheng, S., Zhizhong, P. (1983): Crystal structure of a new phosphatic mineral-qingheiite. *Sci. Sinica, ser. B*, **XXVI**, **8**, 876–884.

Received 26 January 2010
Modified version received 23 February 2010
Accepted 26 March 2010